Control of genetic stability by a new heterochromatin compaction pathway involving the Tip60 histone acetyltransferase

Aude Grézy, Martine Chevillard-Briet, Didier Trouche†, and Fabrice Escaffit†,*
Laboratoire de Biologie Cellulaire et Moléculaire du Contrôle de la Prolifération, Center for Integrative Biology, Université de Toulouse, UPS and CNRS, F-31062 Toulouse, France

ABSTRACT **Pericentric heterochromatin is a highly compacted structure required for accurate chromosome segregation in mitosis. In mammals, it relies on methylation of histone H3K9 by Suv39H enzymes, which provides a docking site for HP1 proteins, therefore mediating heterochromatin compaction. Here we show that, when this normal compaction pathway is defective, the histone acetyltransferase Tip60 is recruited to pericentric heterochromatin, where it mediates acetylation of histone H4K12. Furthermore, in such a context, depletion of Tip60 leads to derepression of satellite transcription, decompaction of pericentric heterochromatin, and defects in chromosome segregation in mitosis. Finally, we show that depletion of BRD2, a double bromodomain–containing protein that binds H4K12ac, phenocopies the Tip60 depletion with respect to heterochromatin decompaction and defects in chromosome segregation. Taking the results together, we identify a new compaction pathway of mammalian pericentric heterochromatin relying on Tip60 that might be dependent on BRD2 recruitment by H4K12 acetylation. We propose that the underexpression of Tip60 observed in many human tumors can promote genetic instability via defective pericentric heterochromatin.**

Monitoring Editor
William P. Tansey
Vanderbilt University

Received: May 27, 2015
Revised: Dec 7, 2015
Accepted: Dec 18, 2015

INTRODUCTION

The structure of mammalian heterochromatin around centromeres, that is, in pericentric regions of each chromosome, plays a central role in genomic integrity: it silences the expression of deleterious sequences, such as transposons; prevents deleterious recombination events that can occur in repeated sequences; and allows correct chromosome segregation (Elgin and Grewal, 2003). Thus the factors involved in the formation of such condensed structures or in their maintenance are crucial for genetic stability. Among these factors, Suv39H1 and Suv39H2 proteins methylate histone H3 on lysine 9, promoting the recruitment of heterochromatin protein 1α (HP1α; Peters *et al.*, 2001) and thus heterochromatin compaction. This heterochromatin compaction is critical for preventing cancer progression: Suv39H-negative cells harbor chromosomal instabilities, and Suv39H deficiency in mice is associated with an increased risk of cancer (Peters *et al.*, 2001). Moreover, negative modulation of Suv39H1 promotes tumorigenesis in breast cancer (Khanal *et al.*, 2013), and its overexpression in animal models can suppress tumor formation (Albacker *et al.*, 2013). Modifications in the expression of HP1 proteins are also very frequent in human cancers (Dialynas *et al.*, 2008). Of interest, sensitivity to therapy-induced senescence, which is a promising strategy for cancer treatment, is clearly linked to Suv39H1 expression (Dorr *et al.*, 2013).

As expected considering the global link between histone acetylation and chromatin relaxation, heterochromatin formation and maintenance largely involve histone deacetylation: first, histones in heterochromatin regions are generally hypoacetylated. Moreover, in yeast, histone deacetylases such as Sir2 and Clr3, participate,

This article was published online ahead of print in MBoC in Press (http://www.molbiolcell.org/cgi/doi/10.1091/mbc.E15-05-0316) on December 23, 2015.

†These authors contributed equally to this work.

A.G. and M.C.B. conceived and performed experiments and interpreted results. F.E. conceived and performed experiments, interpreted results, and cowrote the article. D.T. obtained funding, conceived and interpreted experiments, and cowrote the article.

The authors report no conflict of interest.

*Address correspondence to: Fabrice Escaffit (fabrice.escaffit@univ-tlse3.fr).

Abbreviations used: ChIP, chromatin immunoprecipitation; DDR, DNA damage response pathway; LINE, long intercalated nuclear element; MEF, mouse embryonic fibroblasts; siRNA, small interfering RNA.

sequentially or concomitantly with RNA interference machinery, in the initiation, propagation, and maintenance of pericentric heterochromatin (Maison and Almouzni, 2004; Buscaino *et al.*, 2013). In mammals, treatment of cells with histone deacetylase inhibitors impairs HP1 recruitment to pericentric heterochromatin (Taddei *et al.*, 2001), suggesting that histone deacetylation is required for heterochromatin compaction throughout evolution.

However, some histone acetylation events can participate in pericentric heterochromatin function: heterochromatic regions of polytene chromosomes in *Drosophila* harbor histone H4 acetylated on K12 (Turner *et al.*, 1992). Moreover, in mammalian cells, noncoding RNAs produced from the transcription of repeated pericentric regions, called satellites, play a crucial role in heterochromatin formation (Maison and Almouzni, 2004), suggesting a function for histone acetylation, which is associated with the expression of satellites (see, e.g., Papait *et al.*, 2007).

In *Saccharomyces cerevisiae*, H4K12 is acetylated at telomeres by Esa1 (Clarke *et al.*, 2006). In fission yeast, acetylation of histone H3K4 by the Mst1 histone acetyltransferase is involved in heterochromatin formation by favoring the switch of recruitment between Clr4 (homologue of Suv39H) and Swi6 (HP1α; Xhemalce and Kouzarides, 2010). It is striking that the human homologue of Mst1 and Esa1, the histone acetyltransferase Tip60, is also linked to heterochromatin maintenance: DNA double-strand breaks in heterochromatin are repaired by a specific pathway involving Tip60, which is recruited and activated through the binding of its chromodomain to H3K9me3 (Ayrapetov *et al.*, 2014).

The Tip60 histone acetyltransferase is conserved from yeast to humans (Doyon and Cote, 2004). It acetylates canonical histone H4 and H2A, as well as histone variants H2A.Z and H2A.X (Altaf *et al.*, 2010; Ikura *et al.*, 2015). It belongs to the MYST family and participates in a multimolecular complex called the Tip60 complex in mammals, which contains many other enzymes, including the ATPase p400, which mediates the incorporation of the H2A.Z histone variant in chromatin (Gevry *et al.*, 2007).

Tip60 and its associated proteins participate in transcriptional control, and, consistent with its histone acetyltransferase activity, Tip60 is involved in the activation of specific promoters. However, in a few instances, it was found to mediate transcriptional repression (Ai *et al.*, 2007; Chevillard-Briet *et al.*, 2014), but the role of histone acetylation in this process is largely unclear. Members of the Tip60 complex also participate in genetic stability, since both Tip60 and p400 are important, for example, for the repair of DNA double-strand breaks (Murr *et al.*, 2006; Chailleux *et al.*, 2010; Xu *et al.*, 2010; Courilleau *et al.*, 2012).

Through its action on gene expression and genetic stability, Tip60 participates in growth control. In response to DNA damage, it is required for both cell cycle arrest and apoptosis. It first participates in DNA damage signaling through acetylation of ATM, a kinase central to the response to double-strand breaks (Sun *et al.*, 2005). Moreover, it is an essential cofactor of the p53 tumor suppressor (Berns *et al.*, 2004; Legube *et al.*, 2004), facilitating p53 transcriptional activity but also, through direct acetylation of p53, its targeting to specific promoters (Sykes *et al.*, 2006; Tang *et al.*, 2006; Tyteca *et al.*, 2006). Accordingly, Tip60 is underexpressed in a wide variety of human cancers (Gorrini *et al.*, 2007; Mattera *et al.*, 2009). Moreover, mice heterozygous for Tip60 are more susceptible to myc-induced lymphoma or chemically induced colon cancers (Gorrini *et al.*, 2007; Mattera *et al.*, 2009), indicating that Tip60 is a tumor suppressor. The mechanisms by which it mediates its tumor suppressor functions are not completely clear but were shown to involve the control of the DNA damage response (Gorrini *et al.*, 2007) or of the Wnt signaling pathway (Chevillard-Briet *et al.*, 2014).

In this study, we analyze the role of Tip60 in pericentric heterochromatin maintenance and function in mouse cells. We find that it participates in a new pathway of heterochromatin compaction, which can rely on histone H4K12 acetylation and the recruitment of BRD2, a double bromodomain–containing protein that binds H4K12ac. Taken together, our results demonstrate that mammalian Tip60 can be a major regulator of pericentric heterochromatin dynamics, providing an alternative compaction pathway to ensure genetic stability.

RESULTS

Tip60 acetylates histones at defective pericentric heterochromatin

In the yeast *Schizosaccharomyces pombe*, the Tip60 orthologue was shown to be involved in the maintenance of heterochromatin at the HMR loci, functioning in collaboration with orthologues of Suv39H1 and HP1 proteins (Xhemalce and Kouzarides, 2010). To test whether this is conserved in mammals, we transfected NIH3T3 cells twice 48 h apart with small interfering RNAs (siRNAs) against Tip60. These siRNAs were shown to decrease efficiently Tip60 protein expression (Chevillard-Briet *et al.*, 2014), and we achieved efficient Tip60 mRNA depletion during at least 5 d (Figure 1A). We did not find any effect of Tip60 depletion on satellite expression (Figure 1B), a marker of heterochromatin decompaction, nor on heterochromatin enrichment of the HP1α protein (Figure 1C). In addition, Tip60 depletion did not affect de novo HP1α recruitment measured with a commonly used assay relying on reexpression of Suv39H1 in Suv39H$^{-/-}$ cells (Maison *et al.*, 2011; unpublished data). Taken together, these data indicate that the regulation of HP1 recruitment to heterochromatin by Tip60 is not conserved in mammals.

Of interest, in cells harboring defects in the normal pathway of heterochromatin compaction, such as cells originating from mice deficient in Suv39H proteins or cells treated with DNA methylation inhibitors, pericentric heterochromatin harbors increased levels of H4K12 acetylation (Peters *et al.*, 2001; Boyarchuk *et al.*, 2014). We confirmed this by chromatin immunoprecipitation (ChIP) experiments. Indeed, ChIP with acetylated H4K12 (H4K12ac)-specific antibodies immunoprecipitated much more major satellite sequences from cells derived from Suv39H knockout mice (Suv39H$^{-/-}$ cells) than from cells derived from control mice (Figure 2A). Moreover, treatment of NIH3T3 cells with 5-azacytidine (5-AzaC), which causes a general decrease in DNA methylation leading to disruption of pericentric heterochromatin, also induced an increase in the amount of major satellite sequences immunoprecipitated by the H4K12ac antibody (Figure 2B). Strikingly, in both cases, depletion of Tip60 using a specific siRNA that we previously validated (see Supplemental Figure S1A for siRNA efficiency) led to a decrease in the amount of major satellite sequences immunoprecipitated by the H4K12ac antibody (Figure 2, C and D), indicating that Tip60 expression is required for this acetylation event in both models.

This result led us to test whether Tip60 is recruited to pericentric heterochromatin when the classical heterochromatin compaction pathway is defective. We found, by ChIP experiments, that immunoprecipitation of Tip60 led to the coimmunoprecipitation of major satellite repeats from Suv39H$^{-/-}$ cells (Figure 2E). This precipitation is specific, since it was not observed in the no-antibody control nor on an unrelated genomic sequence from the p53 promoter in the same cells. Taken together, these data indicate that Tip60 is recruited to pericentric heterochromatin in cells derived from Suv39H$^{-/-}$ mice, where it acetylates histone H4K12.

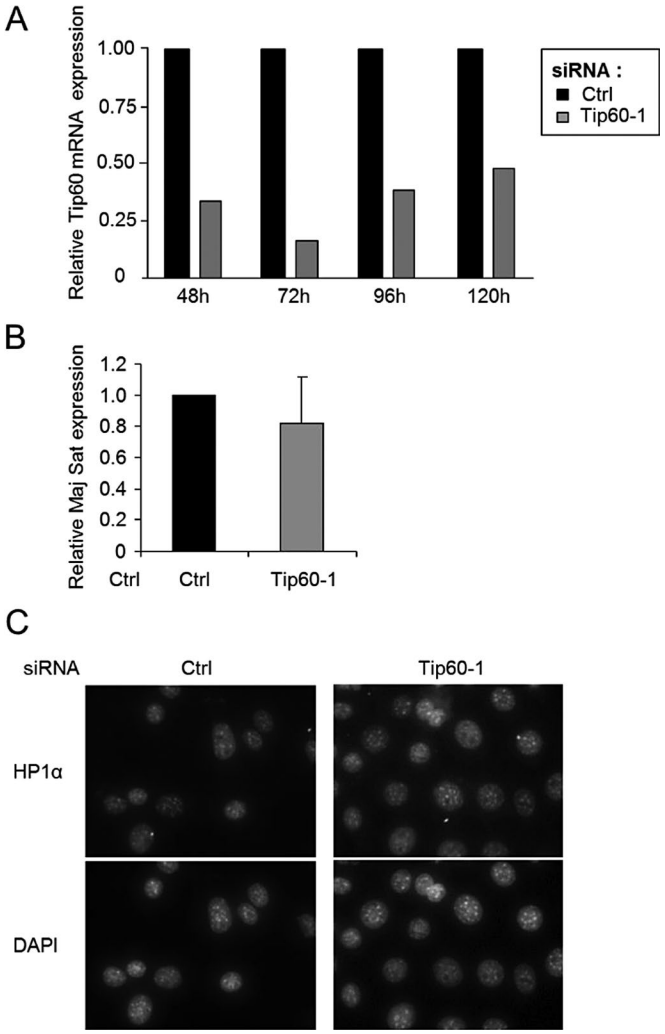

FIGURE 1: Tip60 depletion does not induce any effect on various heterochromatin features in NIH3T3 cells. (A) NIH3T3 cells transfected twice 48 h apart by the indicated siRNA were harvested every 24 h from 48 to 120 h after the first transfection. Tip60 and β2m mRNAs were quantified by reverse transcription, followed by qPCR. The amount of Tip60 mRNA was divided by the amount of β2m mRNA and standardized relative to 1 for cells transfected with control siRNA at each time point. Representative experiment. (B) NIH3T3 cells were transfected using Tip60-1 or control siRNA. The amount of major satellite sequences and β2m mRNA was quantified by reverse transcription, followed by qPCR. The amount of satellite RNA was divided by the amount of β2m mRNA and standardized relative to 1 for cells transfected with control siRNA. Mean and SD from four experiments. (C) NIH3T3 cells transfected twice 48 h apart by the indicated siRNA were fixed 96 h after the first transfection and stained with anti-HP1α antibody and DAPI. Representative images.

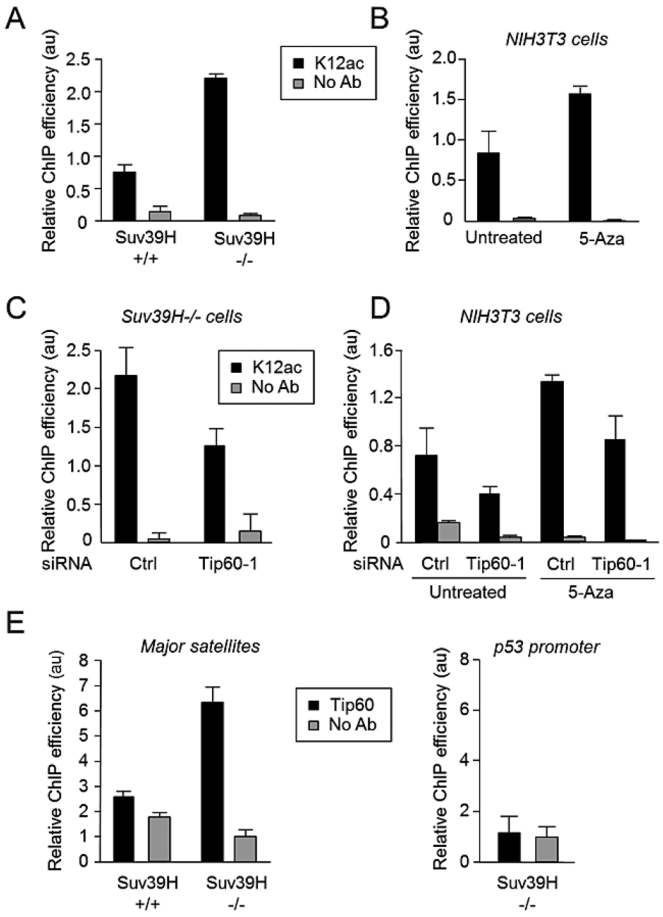

FIGURE 2: Tip60 recruitment to pericentric heterochromatin. (A) Suv39H$^{+/+}$ and Suv39H$^{-/-}$ MEFs were subjected to ChIP assays using anti-H4K12ac antibodies, anti–histone H3 antibody, or no antibody (No Ab) as a control. The presence of major satellite sequences and β2m sequences was quantified by qPCR in the immunoprecipitates and the inputs. The amount of major satellite sequence in the H4K12ac immunoprecipitates was divided by the amount present in the histone H3 immunoprecipitates and standardized relative to β2m sequences. Representative experiment of three. Error bars represent SD within technical triplicates. (B) NIH3T3 treated or not with 5-Aza for 24 h was subjected to a ChIP assay and analyzed as in A. Mean and SD from three experiments. (C) Suv39H$^{-/-}$ cells were transfected with the indicated siRNAs. At 72 h after transfection, cells were subjected to a ChIP assay using anti-H4K12Ac antibodies, anti–histone H3 antibody, or no antibody (No Ab) as a control. The amount of major satellite and β2m sequences was quantified by qPCR in the immunoprecipitates and the inputs as in A. Mean and SD from five independent experiments. (D) NIH3T3 transfected using indicated siRNA was treated or not with 5-Aza 48 h later for 24 h and subjected to a ChIP assay and analyzed as in A. Mean and SD from three independent experiments. (E) Suv39H$^{-/-}$ and Suv39H$^{+/+}$ cells were subjected to a ChIP assay using anti-Tip60 antibody or no antibody (No Ab) as a control. The presence of major satellite sequences as well as p53 promoter was quantified by qPCR in the immunoprecipitates and the inputs. The relative efficiency of the IP from a representative experiment of three is shown relative to 1 for the no-antibody amount in Suv$^{-/-}$ cells. Error bars represent SD within technical triplicates.

Tip60 is important for heterochromatin compaction in Suv39H$^{-/-}$ cells

We next tested the function of Tip60 in pericentric heterochromatin compaction in Suv39H$^{-/-}$ cells. To this end, we transfected Suv39H$^{-/-}$ cells with previously characterized Tip60 siRNAs (Chevillard-Briet *et al.*, 2014) and stained them with 4′,6-diamidino-2-phenylindole (DAPI) to observe heterochromatic foci. We found that Tip60 depletion resulted in cells harboring disrupted foci compared with cells transfected with the control siRNA (Figure 3A). To quantify these changes, we used a plug-in developed in Carl Mann's laboratory to monitor DAPI heterogeneity in cells as a coefficient of variation (DAPI CV; Jeanblanc *et al.*, 2012). This plug-in efficiently detects heterochromatin compaction in senescence-associated heterochromatin

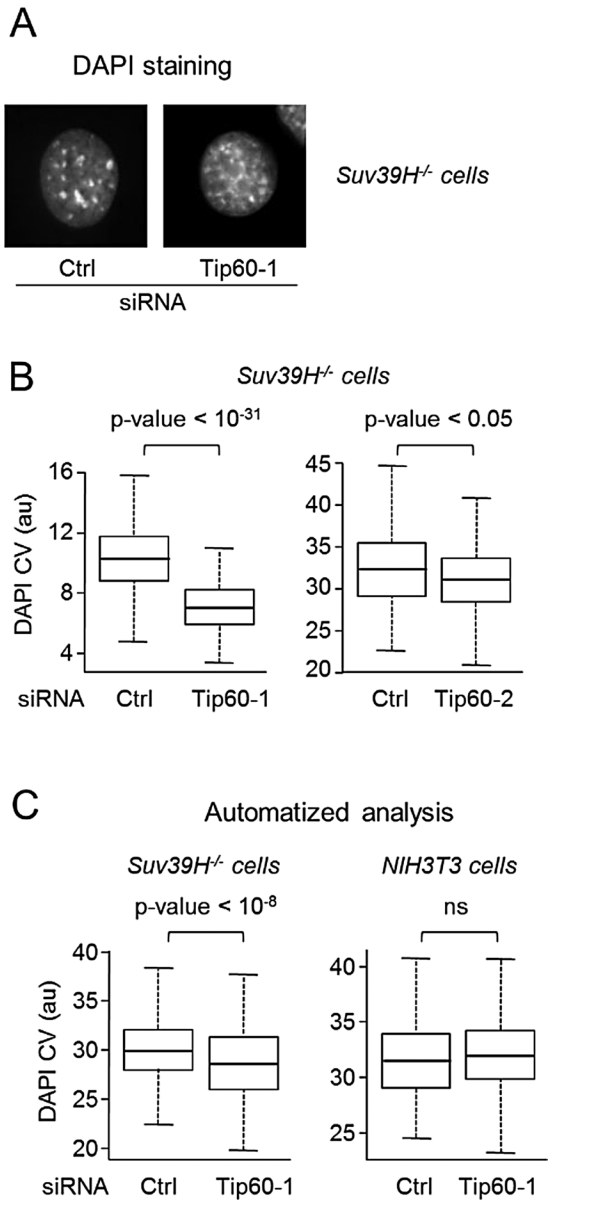

FIGURE 3: Tip60 is involved in heterochromatin compaction. (A) Suv39H$^{-/-}$ cells were transfected using Tip60-1 or control siRNA. At 48 h later, cells were fixed and stained with DAPI. Representative images of cells. (B) Same as in A, except that two Tip60 siRNAs were used and DAPI CV from at least 100 cells by conditions was calculated. Box plots represent the cell population, with the median and the 50 and 75% quantiles. The *p* values of the difference between the two cell populations are indicated above the graphs. Note that raw values of DAPI CV strongly varied from one experiment to another, depending on the settings used for image acquisition. (C) Suv39H$^{-/-}$ and NIH3T3 cells were transfected using Tip60-1 or control siRNA. Cells were seeded in 96-well plates, and 48 h later, cells were fixed and stained with DAPI and then analyzed automatically for DAPI coefficient of variance using the Operetta device.

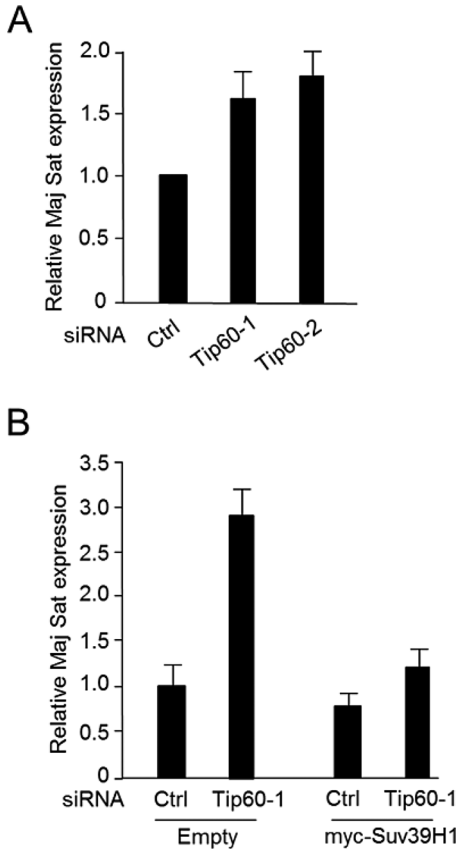

FIGURE 4: Tip60 represses major satellite expression in a Suv39H-deficient context. (A) Suv39H$^{-/-}$ cells were transfected by the indicated siRNA, and 72 h later, cells were harvested and RNA was extracted. The presence of major satellites and β2m RNAs was quantified by reverse transcription, followed by qPCR. The amount of major satellites RNAs was divided by the amount of β2m mRNA and standardized relative to 1 for cells transfected with control siRNA. Mean and SD from four independent experiments. (B) Suv39H$^{-/-}$ cells or cells rescued for Suv39H1 expression were transfected by the indicated siRNA. At 72 h later, cells were harvested, and the amount of major satellite sequences was analyzed as in A. Representative experiment out of three.

foci observed in senescent cells. We found that depletion of Tip60 resulted in a significant decrease of DAPI heterogeneity in Suv39H$^{-/-}$ cells (Figure 3B), reflecting decompaction of heterochromatin. Of importance, we found similar results using two independent siRNAs against Tip60, ruling out off-target effects (for siRNA efficiency, see Supplemental Figure S1A). Using the Operetta platform—a device allowing automatic acquisition and analysis of fluorescence (see *Materials and Methods*)—we confirmed that Tip60 depletion significantly decreased DAPI heterogeneity in Suv39H1$^{-/-}$ cells (Figure 3C) but not wild-type NIH3T3 cells. Taken together, these data indicate that Tip60 is important for heterochromatin compaction in a Suv39H-negative background.

Pericentric heterochromatin decompaction is associated with an increase in the transcription of satellite repeats. Indeed, transcription of pericentric repeats is stimulated in Suv39H-knockout cells and strongly induced upon treatment of cells with 5-AzaC (Gopalakrishnan *et al.*, 2009). We thus monitored the effect of Tip60 depletion on satellite repeat expression. We found that Tip60 depletion using the two specific siRNAs led to an increase in major satellite expression in Suv39H$^{-/-}$ cells (Figure 4A). Moreover, this increase was abolished upon restoration of normal pericentric heterochromatin in these cells by transfection of an expression vector for Suv39H1 (Figure 4B; see Supplemental Figure S1C for Tip60 siRNA efficiency and Suv39H1 expression level). Because this increase was also not seen in wild-type cells, as mentioned earlier (Figure 1), this indicates that Tip60 represses major satellite expression only when the classical heterochromatin compaction pathway is defective.

Note, however, that we did not find any stimulation of major satellite expression after Tip60 knockdown in NIH3T3 cells treated with 5-AzaC (Supplemental Figure S2), probably because heterochromatin decompaction is much more pronounced in this situation and cannot be further increased by Tip60 depletion despite the modulation of H4K12 acetylation seen in Figure 2D.

Taken together, these data indicate that the Tip60 histone acetyltransferase is involved in both the compaction of pericentric heterochromatin and the repression of repeats transcription.

Tip60 deficiency strengthens the genetic-instability phenotype of Suv39H$^{-/-}$ cells

Pericentromeric heterochromatin compaction is important for genetic stability, and satellite overexpression is associated with its relaxation (Ting *et al.*, 2011). As a consequence, Suv39H$^{-/-}$ cells, in addition to satellite-overexpression phenotype, harbor defects in chromosome segregation in mitosis, with the appearance of a general polyploidy (Peters *et al.*, 2001). Because Tip60 depletion further decreases heterochromatin compaction and further increases satellite transcription, we reasoned that it might further increase the genetic-instability phenotypes associated with Suv39H inactivation. We thus transfected Tip60 siRNAs in Suv39H$^{-/-}$ cells and analyzed the presence of hyperpolyploid cells 6 d after transfection. We observed a significant increase in the number of mitotic cells with twice the amount of chromosomes when counted in chromosomes spreads (Figure 5A). We also quantified this phenomenon by propidium iodide staining followed by flow cytometry and we that Tip60 depletion induces an increase in the number of hyperpolyploid Suv39H$^{-/-}$ cells (Figure 5B). Strikingly, this increase was not observed upon Tip60 depletion in wild-type NIH3T3 cells. Thus these data indicate that Tip60 depletion, in a Suv39H$^{-/-}$ context, favors polyploidy. We next analyzed the presence of micronuclei, a feature that is also associated with the inactivation of Suv39H and reflects mitosis defects leading to aneuploidy (Wang *et al.*, 2013). We found that the percentage of cells harboring micronuclei strongly increased upon Tip60 knockdown in Suv39H$^{-/-}$ cells but not in NIH3T3 cells (Figure 5C; see also Supplemental Figure S3 for another Tip60 siRNA).

Taken together, these data indicate that the expression of the Tip60 complex is important for the correct segregation of chromosomes in a Suv39H-depleted context.

Heterochromatin compaction can be mediated by BRD2

We next investigated the molecular mechanism by which Tip60 could mediate the compaction of heterochromatin, an unexpected role for a histone acetyltransferase, given that acetylation is generally associated with chromatin relaxation. Strikingly, proteins with two bromodomains of the BRD family were found to mediate chromatin compaction in an acetylation-dependent manner (Pivot-Pajot *et al.*, 2003). Moreover, BRD2 was previously found to bind to acetylated H4K12 (Umehara *et al.*, 2010), which is the Tip60-dependent histone modification found in pericentric heterochromatin upon Suv39H depletion (see earlier discussion). We thus tested the involvement of BRD2 in Tip60-dependent heterochromatin functions in the Suv39H$^{-/-}$ background. We first found that BRD2 is recruited to pericentric heterochromatin in Suv39H$^{-/-}$ cells, as shown by ChIP experiments (Figure 6A). This recruitment is specific, since enrichment of pericentric sequences was much lower in the no-antibody control. Furthermore, no enrichment of an unrelated sequence from the β2m promoter could be observed in the BRD2 ChIP.

Depletion of BRD2 using a specific siRNA (see Supplemental Figure S1B for the validation of siRNA efficiency) led to the decompaction of heterochromatin in Suv39H$^{-/-}$ cells, as shown by

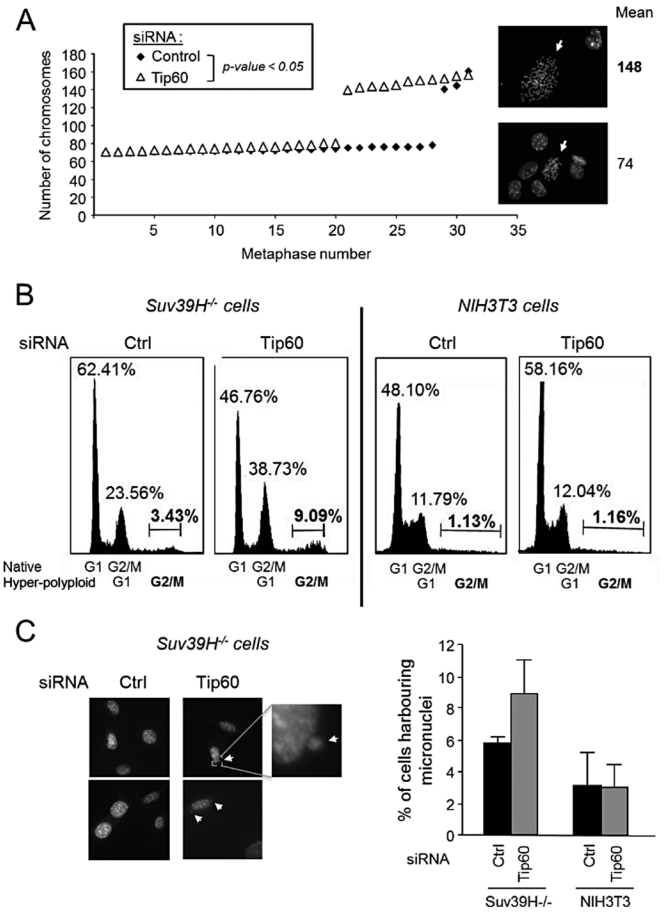

FIGURE 5: Tip60 expression is important for correct chromosome segregation in Suv39H$^{-/-}$ cells. (A) Metaphase spreads of Suv39H$^{-/-}$ cells transfected by the indicated siRNA and blocked in mitosis 6 d later by Colcemid treatment. The number of chromosomes in each metaphase plate is indicated (from 25 to 27 fields, representing 31 metaphases/condition ordered by number of chromosomes). Statistical analysis was performed using chi-squared test. Representative images illustrating cells with single or double chromosome numbers. (B) Suv39H$^{-/-}$ and NIH3T3 cells transfected twice at 48 h apart by the indicated siRNA were harvested 7 d later. Cells were fixed and stained with propidium iodide and analyzed by flow cytometry. (C) Suv39H$^{-/-}$ and NIH3T3 cells were transfected using Tip60 or control siRNA, and 72 h later, cells were fixed and stained with DAPI. Representative images for Suv39H$^{-/-}$ cells. The arrows point toward micronuclei. The graph corresponds to the quantification of three independent experiments with at least 100 cells analyzed by conditions in each experiment. Mean and SD.

DAPI CV measurement, either manually or automatically (Figure 6B). We also observed the appearance of aneuploidy upon BRD2 depletion, as shown by the increase in the number of cells harboring micronuclei (Figure 6C).

Thus these data indicate that BRD2 depletion phenocopies the depletion of Tip60, suggesting that it mediates the Tip60-dependent heterochromatin compaction in Suv39H$^{-/-}$ cells.

DISCUSSION

In this study, we identified a new pathway involved in heterochromatin compaction and function. This pathway can function as a backup pathway important in the absence of the normal Suv39H-HP1α canonical pathway. Indeed, we observe Tip60 recruitment to

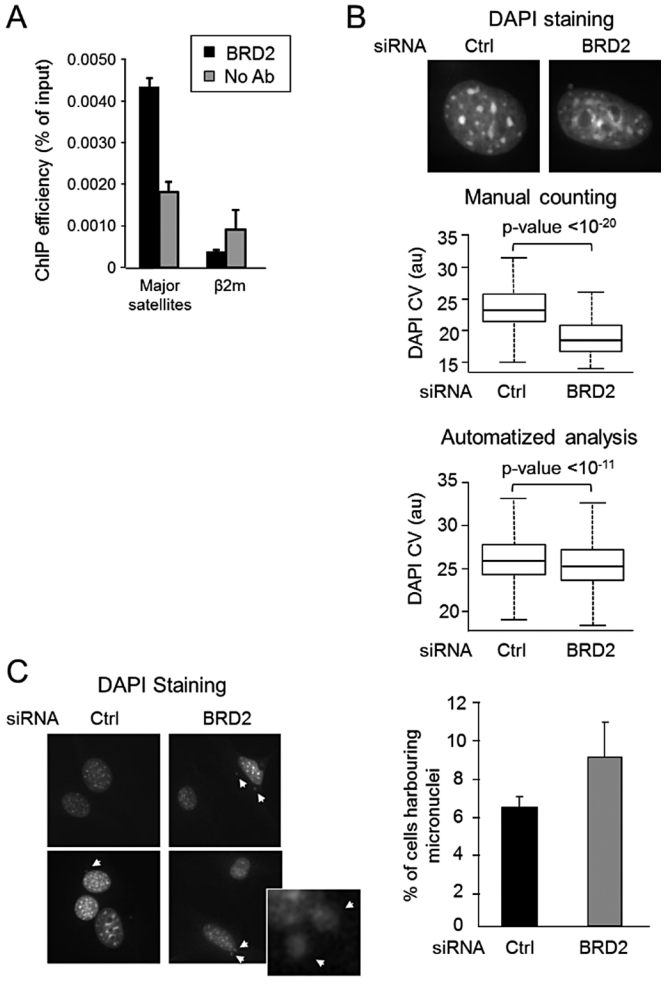

FIGURE 6: Tip60 function in heterochromatin is mediated by BRD2. (A) Suv39H$^{-/-}$ cells were subjected to a ChIP assay using anti-BRD2 antibodies or no antibody (No Ab) as a control. The presence of major satellite and β2m sequences was quantified by qPCR in immunoprecipitates and inputs. Percentage of inputs from a representative experiment out of three. Error bars represent SD within technical triplicates. (B) Suv39H$^{-/-}$ cells were transfected using BRD2 or control siRNA, and 72 h later, cells were fixed and stained with DAPI. Representative images of cells. DAPI CV from at least 100 cells by conditions was calculated manually (DAPI coefficient of variation) or automatically (DAPI coefficient of variance) using the Operetta device. Box plots represent the cell populations, with the median and the 50th and the 75th quantiles. The *p* value of the difference between the two cell populations is indicated above the graphs. (C) Suv39H$^{-/-}$ cells were transfected using BRD2 or control siRNA, and 72 h later, cells were fixed and stained with DAPI. Representative images of cells. The arrows point toward micronuclei. The graph corresponds to the quantification of three independent experiments with at least 100 cells analyzed by conditions in each experiment. Mean and SD.

heterochromatin only in the absence of Suv39H proteins, and it mediates histone H4K12ac, a modification that was previously shown to be specifically enriched in a context in which heterochromatin is abnormal. Moreover, we did not find any effect of Tip60 depletion on heterochromatin transcription in normal cells. Although this is not definitive proof that Tip60 does not play a role in pericentric heterochromatin in normal cells, either because the depletion we achieved is not sufficient or because it is involved in very specific time or space windows (see later discussion), our results indicate that the Tip60-dependent heterochromatin pathway is particularly important when the normal pathway of heterochromatin maintenance is defective. Of interest, we found that Tip60 depletion also leads to overexpression of LINE retroviral sequences in Suv39H$^{-/-}$ cells (Supplemental Figure S4). Because these LINE sequences are also regulated by Suv39H-HP1α (Ting *et al.*, 2011; Bulut-Karslioglu *et al.*, 2014), the pathway we uncover here is probably not restricted to pericentric heterochromatin but can replace the canonical constitutive heterochromatin compaction pathway wherever it is involved.

Our results show that in Suv39H-deficient cells, depletion of Tip60 leads to the strengthening of phenotypes that are associated with defects in pericentric heterochromatin, such as the decompaction of heterochromatin and the increase in the expression of noncoding RNAs produced from heterochromatin sequences. Moreover, it increases the genetic instability associated with heterochromatin dysfunction, with defects in chromosome segregation in mitosis, exemplified by the increase in the percentage of cells harboring micronuclei, as well as of polyploid cells.

Paradoxically, given the known link between histone acetylation and chromatin compaction, our results indicate that a histone acetyltransferase mediates both histone acetylation, at least on H4K12, and chromatin compaction. Of interest, histone acetylation could be directly involved in heterochromatin compaction by allowing the recruitment of BRD2, which belongs to the double bromodomain–containing protein family, some of which are able to mediate the compaction of acetylated chromatin (Pivot-Pajot *et al.*, 2003; Wang *et al.*, 2012). In agreement with this, depletion of BRD2 mimics Tip60 depletion with respect to heterochromatin compaction and chromosome segregation defects.

Note that we were not able to formally demonstrate that BRD2 recruitment was dependent on H4K12 acetylation. We cannot thus rule out the involvement of other mechanisms in Tip60-mediated heterochromatin compaction. Indeed, we did not find any evidence for changes in the expression of pericentric heterochromatin sequences upon BRD2 depletion in these cells (Supplemental Figure S5). This indicates that chromatin decompaction is not sufficient for an increased expression of pericentric repeats, underlining the requirement of acetylation of another substrate (either another histone residue than H4K12 or another protein) by Tip60 to repress satellites expression.

Other questions raised by our findings are where and when this pathway participates in heterochromatin compaction or, in other terms, the physiopathological situation in which it could be involved. First, this could occur during cancer progression. Indeed, most cancers, if not all, have defects in heterochromatin, with decreased DNA methylation (Wilson *et al.*, 2007), in a manner reminiscent of 5-AzaC–treated cells. Moreover, defects in the canonical heterochromatin compaction pathway are common in human cancers (Dialynas *et al.*, 2008; Slee *et al.*, 2011). During the course of cancer progression, it is thus possible that the heterochromatin compaction pathway we uncover here allows cells to maintain a sufficiently accurate chromosome segregation to avoid their elimination by checkpoints or death because of too high a chromosome imbalance. Strikingly, Tip60 is a tumor suppressor often underexpressed in human cancers. Developed cancer may thus harbor defects in both the normal pericentric maintenance pathway and the pathway we identified here. This could lead to high genetic instability, which could further reinforce cancer progression or favor the appearance of drug-resistant clones of cancer cells. Along this line, Tip60 is known to facilitate DNA double-strand break repair (Murr *et al.*, 2006; Chailleux *et al.*, 2010). Moreover, a decrease in Tip60 levels abolishes tumor suppressor pathways such as the DDR and p53 pathways (Berns *et al.*, 2004; Legube *et al.*, 2004; Sun *et al.*, 2005),

eliminating cells with high genetic instability. Tip60 deficiency can thus both increase genetic stability of cancer cells (by decreasing DNA repair efficiency and inducing defects in chromosome segregation; this study) and decrease the mechanism eliminating damaged cells. Such mechanisms probably explain, at least in part, the tumor suppressor functions of Tip60.

The question of whether the heterochromatin compaction pathway we uncovered here is also important in normal cells is an open and important one. In agreement with this, Mst1, the Tip60 orthologue in *S. pombe*, is important for heterochromatin function. Of interest, there are normal situations in which the canonical Suv39H-HP1α heterochromatin compaction pathway is not functional, such as at the very early stage of development in mouse (Santos *et al.*, 2005), as well as in late S phase. In the latter case, recruitment of the demethylase JMJD2A also removes H3K9me3, in a manner very similar to what is seem in Suv39H-depleted cells (Park *et al.*, 2014). Because H4K12ac is associated with telomeric heterochromatin plasticity in *S. cerevisiae* (Zhou *et al.*, 2011), it is tempting to speculate that the pathway we uncovered here is involved in processes requiring heterochromatin plasticity, such as during DNA repair and replication. In agreement with such a hypothesis, Tip60 has been found to be involved in DNA double-strand break repair in heterochromatin (Ayrapetov *et al.*, 2014). Moreover, we found by ChIP using synchronized cells that the level of histone H4K12ac increases during the cell cycle and is maximal in late S phase (Supplemental Figure S6), at a time when transcription of pericentric repeats is decreased (Lu and Gilbert, 2007). Whether Tip60-dependent compaction is functionally important for heterochromatin function and maintenance at this very specific cell cycle stage or during the repair of DNA damage occurring in heterochromatin is a question that clearly merits further investigation.

MATERIALS AND METHODS

Antibodies, vectors, siRNAs, and primers

Anti-H4K12ac and anti-H3 antibodies were purchased from Abcam (Paris, France), and anti-BRD2 was from Bethyl Laboratories (Montgomery, TX). Anti-Tip60 antibody was purchased from Upstate Laboratories (Merck Millipore, Darmstadt, Germany). The myc-Suv39H1 expression vector was a kind gift from T. Jenuwein (Max Planck Institute of Immunobiology and Epigenetics, Freiburg, Germany; Peters *et al.*, 2001).

All siRNAs were purchased from Eurogentec (Angers, France). Sequences were as follows:

Control siRNA: ACUCAAACUCACGAAGGAA-dTdT.

Tip60-1: UGAGAUUGAUGGACGGAAA-dTdT.

Tip60-2: UGAAGAACAUUGAGUGUAU-dTdT.

BRD2 siRNA: GACAAAGGAGGAACUGGCUUUGGAG-dTdT.

The following primers were used:

Tip60 mRNA: 5′-GACCCCTTCCTCTTCTACGT-3′ and 5′-CCGGTCTTCCCTTCTACTTT-3′.

p400 mRNA: 5′-GAAGTTGGCTGCTGCTAAGA-3′ and 5′-CCTCTTCTGGAAACTTTCTG-3′.

Suv39H1 mRNA: 5′-GGGTCCACTTGCATGTTGTAA-3′ and 5′-GGCAACATCTCCCACTTTGT-3′.

Major satellites (expression and ChIP): 5′-GACGACTTGAAAAATGACGAAATC-3′ and 5′-CATATTCCAGGTCCTTCAGTGTGC-3′.

β2m mRNA (expression and ChIP): 5′-CCCGTTCTTCAGCATTTGGA-3′ and 5′- CCGAACATACTGAACTGCTACGTAA-3′.

p53 promoter: 5′-CAGAGCAGAAAGGGACTTGG-3′ and 5′-CTTCACTTGGGCCTTCAAAA-3′.

Cell culture, transfection, and treatments

Mouse embryonic fibroblasts (MEFs) derived from Suv39H$^{-/-}$ or Suv39H$^{+/+}$ animals (kind gifts from T. Jenuwein; Peters *et al.*, 2001) and NIH3T3 cells (ATCC-LCG, Molsheim, France) were cultured in DMEM supplemented with 10% fetal calf serum and antibiotics.

Cells were electroporated with siRNAs (100 µM) or plasmids (1 µg) using an electroporation device (Amaxa AG, Lonza, France), according to manufacturer's specifications. The stable Suv39H1-expressing cell line (named "rescued MEFs") was obtained after selection for 7 d using 2 µg/ml puromycin.

When required, cells were treated using 5-azacytidine (10 µM) for ~24 h before being harvested and used in ChIP experiments.

DAPI staining, metaphase spreads, and flow cytometry analysis

For DAPI staining, cells were fixed with 4% formaldehyde before staining for 3 min with DAPI (Sigma-Aldrich, St Quentin Fallavier, France). Staining was then quantified by counting micronuclei or evaluating chromatin compaction using the DAPI CV quantification plug-in on ImageJ (from C. Mann's laboratory, CEA, Gif-sur-Yvette, France; Contrepois *et al.*, 2012).

In metaphase spread experiments, cells were treated using 0.1 µg/ml Colcemid for 2 h, trypsinized, washed, and then lysed for 25 min in hypotonic solution (75 mM KCl). After addition of fixative solution (ethanol:acetic acid, 3:1), metaphasic plates were then spread on microscope slides, stained with DAPI for 3 min, and photographed.

For flow cytometry analysis, cells were trypsinized, fixed with 70% ethanol, stained with propidium iodide supplemented with RNase (BD Biosciences, Pont-de-Claix, France), and analyzed by flow cytometry. Quantification was done using CellQuest software (BD Biosciences).

Automatic measurement of fluorescence

Automatic high-throughput/high-content analysis was performed using an Operetta device (PerkinElmer, Courtaboeuf, France). Briefly, Suv39H$^{-/-}$ cells were transfected as described and seeded into 96-well plates (Cell Carrier; PerkinElmer) at the density of 5000 cells/well. At 48 h later, cells were fixed and stained with DAPI, also as described, and then observed using the Operetta platform (20× objective, 0.19 numerical aperture; Olympus, Tokyo, Japan). DAPI images were taken for each well in an optimized plane and analyzed for the DAPI coefficient of variance (CV; i.e., SD divided by mean) using a script operated by an integrated software package (Acapella; PerkinElmer).

Data for 500–1000 cells/well were collected, illustrated in box plots, and statistically analyzed with R software. Briefly, for each comparison of microscopy DAPI CV data, we applied the statistical test of Shapiro to determine whether the list of values is normally ($p > 0.05$) or not normally ($p < 0.05$) distributed. Because at least one of the lists was not normally distributed, we applied the Mann–Whitney–Wilcoxon test.

Immunofluorescence

Cells seeded on coverslips were fixed in 4% paraformaldehyde and incubated with primary anti-HP1α and secondary anti-mouse (Euromedex, Souffelweyersheim, France) antibodies before being stained with DAPI, mounted, and observed, as previously described (Escaffit *et al.*, 2007).

RNA extraction, reverse transcription, and quantitative PCR analysis

RNA extraction were performed with TRIzol reagent and then treated with DNase I and DNase Z for 1.5 h at 37°C. DNases were

then precipitated and eliminated with lysis solution and MPC protein precipitation reagent from Epicentre (Tebu-Bio, Le Perrey-en-Yvelines, France). After reverse transcription using random primers and AMV reverse transcriptase (Promega, Madison, WI), quantitative PCR (qPCR) analysis was performed using iQ qPCR mix and a real-time PCR device (Bio-Rad, Marnes-la-Coquette, France) according to the manufacturer's instructions. qPCRs were performed in triplicate.

Chromatin immunoprecipitation

Chromatin immunoprecipitation experiments were performed essentially as described. Briefly, cells were fixed in 1% formaldehyde (15 min), and glycine was added to block the reaction. Nuclei were prepared and sonicated to generate DNA fragments with lengths between 500 and 1500 base pairs. After preclearing and blocking steps, immunoprecipitations were performed overnight with specific antibodies or without antibody as negative control. After centrifugation to eliminate background, recovery of the immune complexes was performed by the incubation of samples with a mixture of blocked protein A/protein G beads (Sigma-Aldrich) on a rotating wheel (1 h at 4°C). After washing, the DNA–protein cross-link was reversed by the addition of RNase A to the samples (30 min at 37°C) and heating under agitation at 70°C overnight. After proteinase K digestion (1.5 h), DNA was purified using a GFX DNA Purification kit (GE Healthcare, Vandoeuvre-les-Nancy, France) and then quantified by qPCR using iQ qPCR mix and a real-time PCR device (Bio-Rad) according to the manufacturer's instructions. qPCRs were performed in triplicate.

ACKNOWLEDGMENTS

We thank Thomas Jenuwein for providing cell models and Saadi Khochbin and all members of the Trouche lab for helpful discussions. We especially thank Catherine Chailleux for technical help in automatized imaging analysis, as well as Marion Aguirrebengoa for statistical analysis of these data. Operetta high-throughput analysis, cytometry, and fluorescence imaging microscopy were performed at the Toulouse Réseau Imagerie TRI facility located at the Laboratoire de Biologie Cellulaire et Moléculaire du Contrôle de la Prolifération. This work was supported by grants from the Fondation ARC to D.T. under Programme ARC and the Agence Nationale de la Recherche. A.G. was supported by a studentship from the Ligue Nationale Contre le Cancer.

REFERENCES

Ai W, Zheng H, Yang X, Liu Y, Wang TC (2007). Tip60 functions as a potential corepressor of KLF4 in regulation of HDC promoter activity. Nucleic Acids Res 35, 6137–6149.

Albacker CE, Storer NY, Langdon EM, Dibiase A, Zhou Y, Langenau DM, Zon LI (2013). The histone methyltransferase SUV39H1 suppresses embryonal rhabdomyosarcoma formation in zebrafish. PLoS One 8, e64969.

Altaf M, Auger A, Monnet-Saksouk J, Brodeur J, Piquet S, Cramet M, Bouchard N, Lacoste N, Utley RT, Gaudreau L, Cote J (2010). NuA4-dependent acetylation of nucleosomal histones H4 and H2A directly stimulates incorporation of H2A.Z by the SWR1 complex. J Biol Chem 285, 15966–15977.

Ayrapetov MK, Gursoy-Yuzugullu O, Xu C, Xu Y, Price BD (2014). DNA double-strand breaks promote methylation of histone H3 on lysine 9 and transient formation of repressive chromatin. Proc Natl Acad Sci USA 111, 9169–9174.

Berns K, Hijmans EM, Mullenders J, Brummelkamp TR, Velds A, Heimerikx M, Kerkhoven RM, Madiredjo M, Nijkamp W, Weigelt B, *et al*. (2004). A large-scale RNAi screen in human cells identifies new components of the p53 pathway. Nature 428, 431–437.

Boyarchuk E, Filipescu D, Vassias I, Cantaloube S, Almouzni G (2014). The histone variant composition of centromeres is controlled by the pericentric heterochromatin state during the cell cycle. J Cell Sci 127, 3347–3359.

Bulut-Karslioglu A, De La Rosa-Velazquez IA, Ramirez F, Barenboim M, Onishi-Seebacher M, Arand J, Galan C, Winter GE, Engist B (2014). Suv39h-dependent H3K9me3 marks intact retrotransposons and silences LINE elements in mouse embryonic stem cells. Mol Cell 55, 277–290.

Buscaino A, Lejeune E, Audergon P, Hamilton G, Pidoux A, Allshire RC (2013). Distinct roles for Sir2 and RNAi in centromeric heterochromatin nucleation, spreading and maintenance. EMBO J 32, 1250–1264.

Chailleux C, Tyteca S, Papin C, Boudsocq F, Puget N, Courilleau C, Grigoriev M, Canitrot Y, Trouche D (2010). Physical interaction between the histone acetyl transferase Tip60 and the DNA double-strand breaks sensor MRN complex. Biochem J 426, 365–371.

Chevillard-Briet M, Quaranta M, Grezy A, Mattera L, Courilleau C, Philippe M, Mercier P, Corpet D, Lough J, Ueda T, *et al*. (2014). Interplay between chromatin-modifying enzymes controls colon cancer progression through Wnt signaling. Hum Mol Genet 23, 2120–2131.

Clarke AS, Samal E, Pillus L (2006). Distinct roles for the essential MYST family HAT Esa1p in transcriptional silencing. Mol Biol Cell 17, 1744–1757.

Contrepois K, Thuret JY, Courbeyrette R, Fenaille F, Mann C (2012). Deacetylation of H4-K16Ac and heterochromatin assembly in senescence. Epigenetics Chromatin 5, 15.

Courilleau C, Chailleux C, Jauneau A, Grimal F, Briois S, Boutet-Robinet E, Boudsocq F, Trouche D, Canitrot Y (2012). The chromatin remodeler p400 ATPase facilitates Rad51-mediated repair of DNA double-strand breaks. J Cell Biol 199, 1067–1081.

Dialynas GK, Vitalini MW, Wallrath LL (2008). Linking heterochromatin protein 1 (HP1) to cancer progression. Mutat Res 647, 13–20.

Dorr JR, Yu Y, Milanovic M, Beuster G, Zasada C, Dabritz JH, Lisec J, Lenze D, Gerhardt A, Schleicher K, *et al*. (2013). Synthetic lethal metabolic targeting of cellular senescence in cancer therapy. Nature 501, 421–425.

Doyon Y, Cote J (2004). The highly conserved and multifunctional NuA4 HAT complex. Curr Opin Genet Dev 14, 147–154.

Elgin SC, Grewal SI (2003). Heterochromatin: silence is golden. Curr Biol 13, R895–R898.

Escaffit F, Vaute O, Chevillard-Briet M, Segui B, Takami Y, Nakayama T, Trouche D (2007). Cleavage and cytoplasmic relocalization of histone deacetylase 3 are important for apoptosis progression. Mol Cell Biol 27, 554–567.

Gevry N, Chan HM, Laflamme L, Livingston DM, Gaudreau L (2007). p21 transcription is regulated by differential localization of histone H2A.Z. Genes Dev 21, 1869–1881.

Gopalakrishnan S, Sullivan BA, Trazzi S, Della Valle G, Robertson KD (2009). DNMT3B interacts with constitutive centromere protein CENP-C to modulate DNA methylation and the histone code at centromeric regions. Hum Mol Genet 18, 3178–3193.

Gorrini C, Squatrito M, Luise C, Syed N, Perna D, Wark L, Martinato F, Sardella D, Verrecchia A, Bennett S, *et al*. (2007). Tip60 is a haploinsufficient tumour suppressor required for an oncogene-induced DNA damage response. Nature 448, 1063–1067.

Ikura M, Furuya K, Matsuda S, Matsuda R, Shima H, Adachi J, Matsuda T, Shiraki T, Ikura T (2015). Acetylation of histone H2AX at Lys 5 by the TIP60 histone acetyltransferase complex is essential for the dynamic binding of NBS1 to damaged chromatin. Mol Cell Biol 35, 4147–4157.

Jeanblanc M, Ragu S, Gey C, Contrepois K, Courbeyrette R, Thuret JY, Mann C (2012). Parallel pathways in RAF-induced senescence and conditions for its reversion. Oncogene 31, 3072–3085.

Khanal P, Kim G, Lim SC, Yun HJ, Lee KY, Choi HK, Choi HS (2013). Prolyl isomerase Pin1 negatively regulates the stability of SUV39H1 to promote tumorigenesis in breast cancer. FASEB J 27, 4606–4618.

Legube G, Linares LK, Tyteca S, Caron C, Scheffner M, Chevillard-Briet M, Trouche D (2004). Role of the histone acetyl transferase Tip60 in the p53 pathway. J Biol Chem 279, 44825–44833.

Lu J, Gilbert DM (2007). Proliferation-dependent and cell cycle regulated transcription of mouse pericentric heterochromatin. J Cell Biol 179, 411–421.

Maison C, Almouzni G (2004). HP1 and the dynamics of heterochromatin maintenance. Nat Rev Mol Cell Biol 5, 296–304.

Maison C, Bailly D, Roche D, Montes de Oca R, Probst AV, Vassias I, Dingli F, Lombard B, Loew D, Quivy JP, Almouzni G (2011). SUMOylation promotes de novo targeting of HP1alpha to pericentric heterochromatin. Nat Genet 43, 220–227.

Mattera L, Escaffit F, Pillaire MJ, Selves J, Tyteca S, Hoffmann JS, Gourraud PA, Chevillard-Briet M, Cazaux C, Trouche D (2009). The p400/Tip60

ratio is critical for colorectal cancer cell proliferation through DNA damage response pathways. Oncogene 28, 1506–1517.
Murr R, Loizou JI, Yang YG, Cuenin C, Li H, Wang ZQ, Herceg Z (2006). Histone acetylation by Trrap-Tip60 modulates loading of repair proteins and repair of DNA double-strand breaks. Nat Cell Biol 8, 91–99.
Papait R, Pistore C, Negri D, Pecoraro D, Cantarini L, Bonapace IM (2007). Np95 is implicated in pericentromeric heterochromatin replication and in major satellite silencing. Mol Biol Cell 18, 1098–1106.
Park SH, Yu SE, Chai YG, Jang YK (2014). CDK2-dependent phosphorylation of Suv39H1 is involved in control of heterochromatin replication during cell cycle progression. Nucleic Acids Res 42, 6196–6207.
Peters AH, O'Carroll D, Scherthan H, Mechtler K, Sauer S, Schofer C, Weipoltshammer K, Pagani M, Lachner M, Kohlmaier A, *et al*. (2001). Loss of the Suv39h histone methyltransferases impairs mammalian heterochromatin and genome stability. Cell 107, 323–337.
Pivot-Pajot C, Caron C, Govin J, Vion A, Rousseaux S, Khochbin S (2003). Acetylation-dependent chromatin reorganization by BRDT, a testis-specific bromodomain-containing protein. Mol Cell Biol 23, 5354–5365.
Santos F, Peters AH, Otte AP, Reik W, Dean W (2005). Dynamic chromatin modifications characterise the first cell cycle in mouse embryos. Dev Biol 280, 225–236.
Slee RB, Steiner CM, Herbert BS, Vance GH, Hickey RJ, Schwarz T, Christan S, Radovich M, Schneider BP, Schindelhauer D, Grimes BR (2011). Cancer-associated alteration of pericentromeric heterochromatin may contribute to chromosome instability. Oncogene 31, 3244–3253.
Sun Y, Jiang X, Chen S, Fernandes N, Price BD (2005). A role for the Tip60 histone acetyltransferase in the acetylation and activation of ATM. Proc Natl Acad Sci USA 102, 13182–13187.
Sykes SM, Mellert HS, Holbert MA, Li K, Marmorstein R, Lane WS, McMahon SB (2006). Acetylation of the p53 DNA-binding domain regulates apoptosis induction. Mol Cell 24, 841–851.
Taddei A, Maison C, Roche D, Almouzni G (2001). Reversible disruption of pericentric heterochromatin and centromere function by inhibiting deacetylases. Nat Cell Biol 3, 114–120.
Tang Y, Luo J, Zhang W, Gu W (2006). Tip60-dependent acetylation of p53 modulates the decision between cell-cycle arrest and apoptosis. Mol Cell 24, 827–839.
Ting DT, Lipson D, Paul S, Brannigan BW, Akhavanfard S, Coffman EJ, Contino G, Deshpande V, Iafrate AJ, Letovsky S, *et al*. (2011). Aberrant overexpression of satellite repeats in pancreatic and other epithelial cancers. Science 331, 593–596.
Turner BM, Birley AJ, Lavender J (1992). Histone H4 isoforms acetylated at specific lysine residues define individual chromosomes and chromatin domains in Drosophila polytene nuclei. Cell 69, 375–384.
Tyteca S, Legube G, Trouche D (2006). To die or not to die: a HAT trick. Mol Cell 24, 807–808.
Umehara T, Nakamura Y, Wakamori M, Ozato K, Yokoyama S, Padmanabhan B (2010). Structural implications for K5/K12-di-acetylated histone H4 recognition by the second bromodomain of BRD2. FEBS Lett 584, 3901–3908.
Wang D, Zhou J, Liu X, Lu D, Shen C, Du Y, Wei FZ, Song B, Lu X, Yu Y, *et al*. (2013). Methylation of SUV39H1 by SET7/9 results in heterochromatin relaxation and genome instability. Proc Natl Acad Sci USA 110, 5516–5521.
Wang R, Li Q, Helfer CM, Jiao J, You J (2012). Bromodomain protein Brd4 associated with acetylated chromatin is important for maintenance of higher-order chromatin structure. J Biol Chem 287, 10738–10752.
Wilson AS, Power BE, Molloy PL (2007). DNA hypomethylation and human diseases. Biochim Biophys Acta 1775, 138–162.
Xhemalce B, Kouzarides T (2010). A chromodomain switch mediated by histone H3 Lys 4 acetylation regulates heterochromatin assembly. Genes Dev 24, 647–652.
Xu Y, Sun Y, Jiang X, Ayrapetov MK, Moskwa P, Yang S, Weinstock DM, Price BD (2010). The p400 ATPase regulates nucleosome stability and chromatin ubiquitination during DNA repair. J Cell Biol 191, 31–43.
Zhou BO, Wang SS, Zhang Y, Fu XH, Dang W, Lenzmeier BA, Zhou JQ (2011). Histone H4 lysine 12 acetylation regulates telomeric heterochromatin plasticity in Saccharomyces cerevisiae. PLoS Genet 7, e1001272.